An MRA Based MLR Model for Forecasting Indian Annual Rainfall Using Large Scale Climate Indices

Abstract

Rainfall forecasting is useful for water resource management and agricultural planning. Annual rainfall is most likely to be influenced by large weather indicators. Therefore, an annual rainfall series and long-term climate indices are decomposed using Multiple Resolution Analysis (MRA) into a certain number of component sub series at different temporal scales. A Multiple Linear Regression (MLR) has then been implemented using climate indices sub-series as predictive variables with a step wise linear regression algorithm. This MRA-based rainfall forecasting method is tested on the annual Indian rainfall and is compared with the traditional MLR model. The outperformance of the proposed model has been proved by relative absolute error and correlation coefficient metrices.

Key Words: *climate indices; forecasting; MLR; MRA; rainfall; time series*

1. Introduction:

Timely and abundant amount of rainfall increase agricultural productivity which ensures food security for the citizens of a country. Agricultural productivity and quality water supply can be safeguarded by efficient rainfall prediction mechanism. However, scarcity of rainfall has a negative impact also to aquatic ecosystem. Agriculture, water quality and aquatic ecosystem are highly correlated with daily and annual rainfall amount (Kusiak et al. 2012).

MRA refers to the processing of any image or signal where signal is processed at multiple resolutions. An MRA or Multiscale Approximation (MSA) technique indicates the practically useful Discrete Wavelet Transforms (DWT). Some of the most commonly used transformations include the Daubechies family, Symlet, B-Splines, Gabor, Coiflet, Meyer etc. (Daubechies 1992). One of the advantages inherent in understanding the idea of wavelets is that unlike Fourier analysis, one can create his own wavelet function to accommodate particular signal (s) of interest. However, it was firstly suggested by Stephane Mallat (Mallat 1989). It is mainly based on the pyramid methods of signal processing as introduced by Burt and Adelson (Burt and Adelson 1983, 1987). Nevertheless, It Decomposes a time series into wavelet domain, alter the wavelet coefficients accordingly for denoising, compression, edge enhancement, etc. and then reconstruct the image with the altered wavelet coefficients. Linear regression methodology can be conceptualized in multivariate level (Makridakis et al. 1982).

This is considered as supervised learning algorithm to predict or forecast unknown dependent variable based on the known features or independent variables (Draper and Smith 1998). We can decompose the series of values of response and explanatory variables using MRA and use this information in the MLR model to get accurate prediction for response variable. The above two knowledges can be combined to estimate any variable. Instead of using the variables directly in the multiple regression model, firstly we can decompose those variables applying MRA in different temporal time scales to effectively utilize the information contained in the data set. After that decomposed subseries can be used as potential predictor variables to estimate the response variable.

Accuracy of forecasts of precipitation for periods of large anomalies is more important than that of a normal precipitation period (Schneider and Garbrecht 2003). Change in rainfall pattern is likely relevant to large-scale climate variabilities, and maybe to global warming as well (Ummenhofer et al. 2009). However, Past methods of forecasting rainfall can be broadly classified into two categories: empirical and dynamical. The dynamical models such as general circulation models (GCMs) are conformed with the laws of physics, which have been used to forecast climate variables (Lim et al. 2009; DelSole and Shukla 2012; Schepen et al. 2012). Whereas, the empirical models are based on observational relationships of the predictand variable with various predictors. Unknown parameters are to be determined by regression or other optimization methods from the data (Sahai et al. 2000). GCM models are less accurate and complex. Wherefor Empirical methods are still the most widely used approaches for forecasting seasonal precipitation. Even so they are used in agricultural planning (Meinke and Stone 2005). The empirical methods include statistical models (Mutai et al. 1998; Prasad et al. 2010) and Machine Learning (ML) algorithms (Sahai et al. 2000). As a result of weakened correlation between precipitation and predictor variables with an increasing lag, forecast time is generally 1 to 3 years.

Generally, most rainfall forecasting models use only a set of climate-related variables or historical rainfall data as input. Rather in the rainfall forecast models a combination of historical rainfall data and other climatic attributes can be used simultaneously. Furthermore, some studies have shown that the variability of Indian rainfall has been linked to several dominant large-scale climate signals. They include El Ni˜no Southern Oscillation (ENSO) (Agilan and Umamahesh 2018), Indian Ocean Dipole (IOD) (Karumuri and Saji 2007), Pacific Decadal Oscillation (PDO) (Krishnamurthy and Krishnamurthy 2014). Precipitation

often operate under a large range of temporal scales varying from one day to several decades (Tessier et al. 1996). However, for any rainfall prediction model, these buried relationships on different temporal scales are sources of useful information for predictability.

Sharma (Sharma 2000) provided non-parametric approach for rainfall forecasting to improve management of water supply. Archer and Fowler (Archer and Fowler 2008) utilized meteorological data to predict seasonal run off. Yucel et al. (Yucel et al. 2015) utilized satellite data to improve calibration and evaluation related to flood forecasting. Thirumalai et al. (Thirumalai et al. 2017) utilized several climatic attributes, viz, solar radiation, humidity, etc. to describe rainfall and modelled it using linear regression. Several authors identified various atmospheric features like air pressure, air temperature, wind speed, relative humidity etc. to accurately model rainfall using distinctive ML algorithms including MLR (Diez-Sierra and del Jesus 2017; Basha et al. 2020; Vijayan et al. 2020). They also concluded that deep learning models can be viable alternatives for modelling and forecasting rainfall. Fahimi et al. (Fahimi et al. 2017) studied and applied ANN based hybrid algorithms to model hydrological variables. Paul and Anjoy (Paul and Anjoy 2018) modelled temperature series (maximum) in occurrence of mechanical disruption. Liyew and Melese (Liyew and Melese 2021) utilized MLR algorithm to predict daily rainfall amount utilizing various environmental components. Coon et al. (Coon and Shuai 2022) provided Watershed Workflow toolset (version 1.2) to bridge the mound the gap between available data and available hydrological models. Several authors provided insights about the prediction of ground water table in agricultural areas (Zhang et al. 2018; Jeong et al. 2020), seasonal run off (Gao et al. 2020), drought (Singh et al. 2021) and soil moisture decline (Jia et al. 2017) using several deep machine learning models including copula analysis. Buttinger-Kreuzhuber et al. (Buttinger-Kreuzhuber et al. 2022) proved higher efficiency of Graphics Processing Unit (GPU) integration in simulating flash floods of large urban area at higher resolution over Central Processing Unit (CPU) implementation.

Ghosh et al. (Ghosh et al. 2010) utilized DWT and MRA approaches to find the trend in rainfall data by using Daubechies (D4) and Haar filters at various scales. Jeong et al. (Jeong et al. 2012) proposed monthly rainfall forecasting by neuro fuzzy model. Kim et al. (Kim et al. 2014) integrated the idea of autoregressive models, fuzzy models and Wavelet Transform (WT) to predict algal bloom. They utilized several water quality parameters like total oxygen, pH, Biological Oxygen Demand (BOD), total nitrogen, water outflow, etc. to predict

chlorophyll-a as an indicator of algal bloom. Likewise, annual rainfall can be forecasted using the same concept. Paul and Birthal (Paul and Birthal 2016) employed wavelet approach to find rainfall trend over India and its agro-climatic zones. They concluded that there was no overall trend in Indian rainfall but there were changes in rainfall pattern in certain agroclimatic zones during 1901-2002. Ray et al. (Ray et al. 2020) proposed wavelet based-ANN and Wavelet Neural Network (WNN) to forecast rainfall in India. Jiang et al. (Jiang et al. 2020) applied wavelet-based variance transform technique to downscale Standardized Precipitation Index (SPI12) in Australia to predict drought as response variable. They also to took help of synthetic data to prove that the refined spectral representation can select additional predictors by finding their capability to characterize the residuals obtained from the fitting of original response and predefined predictors. Through sensitivity analysis, Bajirao et al. (Bajirao et al. 2021) found that previous day runoff is the most significant input for predicting daily run off. They also found that wavelet based soft computing tools viz, ANN and Adaptive Neuro Fuzzy Inference System (ANFIS) are more efficient than standalone tools in projecting daily runoff. Among different wavelet filters used in their study Coiflet was the best. Jiang et al. (Jiang et al. 2021) predicted drought anomalies incorporating wavelet-based approach with predictive K-Nearest Neighbors (KNN) model Be that as it may, production of an agricultural crop is dependent on the total cultivated area under the crop, climatic factors like rainfall, temperature, price of different agricultural inputs etc. This information can be utilized to forecast the time series of production of the crop after decomposition into multiple time scale. This additional information will improve the accuracy of forecasting future values of key variable like agricultural produces or prices (Paul and Garai 2021, 2022; Garai and Paul 2023) than the traditional model of forecasting where the lag relationship of the time series is utilized only. Therefore, rainfall prediction is also considered an important study area and indirectly related to agricultural produces and prices. Hence, Quilty and Adamowski (Quilty and Adamowski 2021) integrated wavelet data driven framework with MODWT and Maximum Overlap Discrete Wavelet Packet Transform (MODWPT) to forecast streamflow, precipitation etc. which change over multiple timescales. Karbasi et al. (Karbasi et al. 2022) proved the efficacy of Discrete Meyer (DMeyer) mother wavelet when combined with various ML models to forecast multi-scale Standardized Precipitation and Evapotranspiration Index (SPEI) over other used wavelets.

In order to optimally utilize the information contained in the data, an MRA based on the WT is employed. An effective rainfall forecasting model from the historical rainfall data and

climate signals by incorporating the MRA and multiple linear regression (MLR) model has been developed in this article. It will be examined whether historical precipitation and large-scale climate signals are useful in annual rainfall forecasting in an area of a range of climate types and a big precipitation gradient.

2. Methodology

2.1. MLR

Generally, any particular response variable can be described by many influential variables. Moreover, MLR attempts to find the underlying relationship between the explanatory variables (X) and a response variable (Y) to fit a linear equation to the observed data. Every single value of X is associated with a value of Y. An MLR model with k predictor variables $X_1, X_2, \ldots, X_k$ and a response Y, can be written as:

$$y = \beta 0 + \beta_1 x1 + \beta_2 x_2 + \cdots + \beta_k x_k \quad (1)$$

β_0, β_1, β_2, ..., β_k mentioned in the model are regression coefficients, need to be estimated (de Andrade Lima Neto et al. 2021).

2.2. Wavelet-based approach

A wavelet is a mathematical function useful in digital signal processing and image compression . Although the theory is not new, the principles are similar to those of Fourier analysis. Wavelet is a 'small wave'. A small wave grows and decays essentially in a limited time period. The contrasting notion is obviously a 'big wave'. An example of big wave is the sine function, which keeps on oscillating up and down on a plot of $\sin(u)$ versus $u \in (-\infty, +\infty)$. To begin to quantify the notion of a wavelet, let us consider a real-valued function $\psi(.)$ defined over the real axis $(-\infty, +\infty)$ satisfying two basic properties:

(i) The integral of $\psi(.)$ is zero:

$$\int_{-\infty}^{+\infty} \psi(u) du = 0 \quad (2)$$

(ii) The square of $\psi(.)$ integrates to unity:

$$\int_{-\infty}^{+\infty} \psi^2(u)\, du = 1 \quad (3)$$

If Equation (ii) holds then for any ϵ satisfying $0 < \epsilon < 1$, there must be an interval $[-T, T]$ of finite length such that

$$\int_{-T}^{+T} \psi^2(u)\, du > 1 - \epsilon. \quad (4)$$

If we think of ϵ as being very close to zero, then $\psi(.)$ can only deviate insignificantly from zero outside of [-T, T] (equation 4). Since the length of the interval [-T, T] is vanishingly small compared to the infinite length of the entire real axis$(-\infty, +\infty)$,the non-zero activity of $\psi(.)$ can be considered as limited to relatively small interval of time. While equation (3) tells us that $\psi(.)$ Has to make some excursions away from zero, equation (2) says that any excursions it makes above zero must be cleared away from zero, so $\psi(.)$ Must resemble a wave. Hence equations (2), equation (3), and equation (4) lead to a 'small wave' or wavelet. One important and common additional condition, namely, the so-called admissibility condition (equation 6) should also be satisfied along with the above-mentioned ones. A wavelet $\psi(.)$ is said to be admissible if its Fourier transform (equation 5), namely,

$$\psi(f) \equiv \int_0^{\infty} \psi(u)\, e^{-i2\pi fu}\, du \tag{5}$$

is such that

$$C_{\psi} \equiv \int_0^{\infty} \frac{|\boldsymbol{\psi}(\mathbf{f})|^2}{f} df;\ 0 < C_{\psi} < \infty \tag{6}$$

2.2.1. WT

The WT is a mathematical technique introduced in signal analysis in early 1980s (Goupillaud et al. 1984). It is a method based on expressing signals as sums of little waves. The basic idea of the WT is the decomposition of a signal at different time scales onto a set of basic functions. The set of basic functions $\{\psi_{a,b}(t)\}$ (equation 7) can be generated by translating and scaling the wavelet function $\psi(t)$, called the mother wavelet. According to Daubechies (1992):

$$\psi_{a,b}(t) = (1/\sqrt{a})[\psi(t-b)/a],\ a > 0,\ -\infty < b < \infty \tag{7}$$

Where a is the scale parameter which adjusts the dilation of the wavelet and b determines the location of the wavelet. The mother wavelet $\psi(t)$ satisfies two basic properties of wavelet mentioned above in equation (2), and equation (3). There have been two mainstreams of wavelets. The first one is known as the Continuous Wavelet Transform (CWT), which is designed to work with time series defined over the entire real axis producing redundant amount of subseries; and the second one is the Discrete Wavelet Transform (DWT), which deals with series defined essentially over a range of integers (usually $t = 0,1,2,\ldots,N-1$; where N denotes the number of observations in the series). If $\{\psi(t)\}$ satisfies equation (1), for a finite time series or energy signal $f(t)$, CWT (equation 8) is defined as

$$W_{\psi}(a,b) = \frac{1}{\sqrt{a}} \int_{-\infty}^{+\infty} \overline{\psi}\left(\frac{t-b}{a}\right) f(t)\, dt \tag{8}$$

Where $\bar{\psi}$ is the mother wavelet complex conjugate. For each scale a, the WT result is a set of coefficients associated with different locations b (Lindsay et al. 1996). The continuous wavelet is often discretized to deal with discrete signals in real application. The DWT can be thought as dyadic (concepts of two parts) sampling of $W_{\psi}(a, b)$, in which the mother wavelet is scaled by powers of two, $a = 2^j$ and, within a given scale, translated by integers, $b = k2^j$, where k is a location index and j is referred to as the decomposition level. Thus, from equation (7), a discretely scaled and translated wavelet (equation 9) is expressed as

$$\psi_{j,k}(t) = 2^{-j/2}\psi(2^{-j}t - k) \quad (9)$$

and the the DWT of $f(t)$ can be written as in equation (10)

$$W_{\psi_{j,k}(t)} = 2^{-j/2}\int_{-\infty}^{+\infty}\bar{\psi}(2^{-j}t - k)f(t)\,dt; j = 0, 1, 2, \ldots; k \in \mathbf{Z} \quad (10)$$

The characteristics of the original time series $f(t)$ at the decomposition level j and time location index k at the same time are reflected by $W_{\psi_{j,k}(t)}$. When the time domain resolution of WT is high, j becomes small. As the level and the scale decrease, the time domain resolution increases and the smaller and finer components of the signal can be accessed.

2.2.2. MRA

MRA based on DWT is to decompose the signal with different frequencies into a certain number of component time series at different temporal scales. In order to perform the MRA, the DWT is implemented in a hierarchical algorithm, well known as the pyramid algorithm (Figure 1) (Mallat 1989). The MRA decomposes the signal into different scales by successively translating and convolving the elements of a high-pass filter (which passes signals with a frequency higher than a certain cutoff frequency and attenuates signals with frequencies lower than the cutoff frequency) and low-pass scaling filter (which rejects all unwanted higher frequencies of signals) associated with the mother wavelet (Primer et al. 1998; Percival and Walden 2000). These filters retain the small-and large-scale components of the signals respectively (Mart'inez and Gilabert 2009), also known as detail (D) (equation 11) and approximation (A) (equation 12) subseries. For a particular decomposition level j, the sum of the products of the wavelets and their coefficients for the signal $f(t)$ over all locations (but for one value of the scale parameter 2^j) results in the detail component D_j, i.e.,

$$D_j(t) = \sum_{k=-\infty}^{\infty} W_{\psi_{j,k}}\,\psi_{j,k}(t) \quad (11)$$

Beside the detail component, it also results in a smoothed representation of the signal for scale 2^j, also known as approximation component A_j and described as (Percival and Walden, 2000):

$$A_j(t) = \sum_{k=-\infty}^{\infty} V_{\phi_{j,k}} \phi_{j,k}(t) \quad (12)$$

Where $\phi_{j,k}(t)$ is a scaled and translated basis function, called the scaling function, which is given together with the wavelet function when a wavelet is chosen. $V_{\phi_{j,k}}$ is the scaling coefficient calculated from $\phi_{j,k}(t)$ in a similar way for the wavelet coefficient $W_{\psi_{j,k}}$ from $\psi_{j,k}(t)$. The signal $f(t)$ can be reconstructed from the approximation and detail components as in equation 13:

$$f(t) = D_1(t) + D_2(t) + \ldots + D_j(t) + A_j(t) \quad (13)$$

Where J is the highest decomposition level considered. In the first level of the decomposition, $f(t) = D_1(t) + A_1(t)$, the signal has a low-pass filtered component A_1, and a high-pass filtered component D_1. The same procedure is performed on A_1 in order to obtain a decomposition at coarser scales, $A_1 = D_2 + A_2$. The process is continued in such a way that $A_j = D_{j+1} + A_{j+1}$ for $j = 2, \ldots, J-1$. This is known as famous pyramid algorithm depicted in the Figure 1.

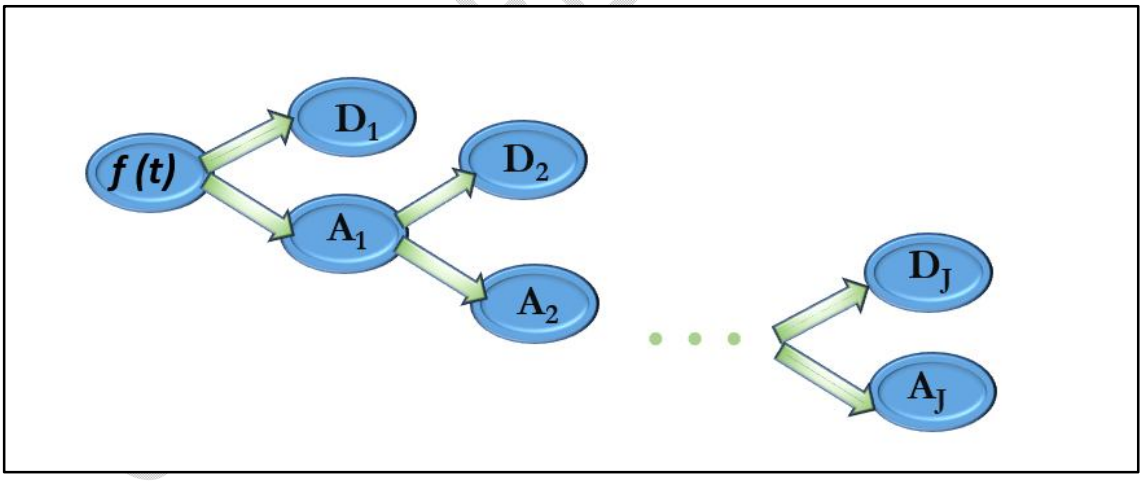

Figure 1: Pyramid Algorithm

2.3. Lag time estimates:

We may assume that rainfall responds to large-scale climate signals with a time lag in this study. Cross correlation between the two sets of signals are calculated for the lag relationship. The lag time estimation is determined by finding the time shift resulting in a maximum cross correlation. All monthly time series are decomposed using the MRA into a certain number of

subseries components under different temporal scales. The lag correlation coefficients (LCC) are measured between rainfall subseries versus each potential predictor subseries (equation 14). Let $y_s(t_n)$ denote the rainfall subseries, and $x_s(t_n - \tau)$) denote the lagged rainfall or largescale climate index subseries, where $n = 0, 1, \ldots, N; t_n = t_0 + n \Delta t$; t_0 is the offset, and Δt is the sampling interval. The lag correlation coefficient between $y_s(t_n)$ and $x_s(t_n)$ is defined as

$$LCC(\tau) = \frac{\left|\sum_{n=\tau}^{N}[y_s(t_n)-\bar{y_s}][x_s(t_{n-\tau})-\bar{x_s}]\right|}{\sqrt{\sum_{n=\tau}^{N}[y_s(t_n)-\bar{y_s}]^2 \sum_{n=\tau}^{N}[x_s(t_{n-\tau})-\bar{x_s}]^2}} \quad (14)$$

where $\bar{y_s}$ and $\bar{x_s}$ stand for the mean of $y_s(t_n)$ and $x_s(t_{n-\tau})$, respectively, and $\tau = 1, 2, \ldots$ Here, in order to forecast rainfall in advance, we take $\tau \geq 1$. The lag time between the subseries $y_s(t_n)$ and $x_s(t_{n)}$ is found from the peak of $LCC(\tau)$. The lag time between the original rainfall series $y(t_n)$ and predictor series $x(t_{n)}$ can be found similarly. By doing this, an optimal time lag is determined for each potential predictor variable for further developing rainfall forecasting models. This is different from some other methods in which time series of different lags are included in the model optimisation stage, as discussed in Beriro et al. (Beriro et al. 2012).

2.4. Proposed models for rainfall forecasting

After the lag relation between rainfall and each candidate predictor is identified, two types of MLR models can be constructed which are discussed below:

2.4.1. Traditional Multiple Linear Regression (TMLR) models

Model based on original rainfall series and climate signal series is the TMLR model (equation 15) given as

$$\hat{y}(t_n) = a_0 + a_1 x_1(t_{n-\tau_1}) + \cdots + a_i x_i(t_{n-\tau_i}) + \cdots + a_I x_I(t_{n-\tau_I}) \quad (15)$$

where $\hat{y}(t_n)$ is the forecasted rainfall value, x_i $(i = 1, \ldots, I)$ are the potential predictors including HRA and large-scale climate indices, $\tau_i \geq 1$ is the lag time between rainfall and the i^{th} predictor, and a_i is the model regression parameter. The a_i values are estimated from the training period data, i.e., (1901-1995). In order to prevent overfitting, and to find the optimal (final) regression model, a stepwise regression algorithm (Draper and Smith 1998) is employed to select significant predictors from all the candidate variables in this study. Finally, the forecasted rainfall values are computed.

2.4.2. Wavelet-based Multiple Linear Regression (WMLR) models

Model based on wavelet-decomposed subseries of the predictor series is WMLR model. The WMLR is constructed by incorporating two methods, MLR and MRA with DWT. For the WMLR model inputs, each of the original rainfall and climate index time series are decomposed into a certain number of subseries components A_J and D's by the MRA. Then the forecasted value of the approximation component of the rainfall in the highest decomposition level J, i.e., $\widehat{A_J^y}(t_n)$ can be obtained by equation 16:

$$\widehat{A_J^y}(t_n) = a_{J,1} + a_{J,2}A_J^{x_1}\left(t_{n-\varsigma_{J,1}}\right) + \cdots + a_{J,i}A_J^{x_i}\left(t_{n-\varsigma_{J,i}}\right) + \cdots + a_{J,I}A_J^{x_I}\left(t_{n-\varsigma_{J,I}}\right) \quad (16)$$

Where $A_J^{x_i}$ $(i = 1, 2, 3 \ldots I)$ are the approximation components of the potential predictor variables x_i $(i = 1, \ldots, I)$ at the highest decomposition level J, $a_{J,i}$ is the regression parameter which can be estimated from the training period data, and $\varsigma_{J,i}, i \geq 1$ is the lag time between the rainfall subseries A_J^y and predictor subseries $A_J^{x_i}$. Similarly, the forecasted value of the detail components of the rainfall series at each decomposition level j, i.e., $D_j^y(t_n)$ $(j = 1, \ldots, J)$ can be expressed as equation 17:

$$\widehat{D_j^y}(t_n) = d_{j,1} + d_{j,2}D_j^{x_1}\left(t_{n-\tau_{j,1}}\right) + \cdots + d_{j,i}D_j^{x_i}\left(t_{n-\tau_{j,i}}\right) + \cdots + d_{j,I}D_j^{x_I}\left(t_{n-\tau_{j,I}}\right) \quad (17)$$

where $D_J^{x_i}$ $(i = 1, \ldots, I)$ is the detail components of the potential predictor x_i at the decomposition level j, and $d_{j,i}$ and $\tau_{j,i} \geq 1$ are the regression parameter and the time lag, respectively. From equations (13), equation (16) and equation (17), we can get the forecasted value of the rainfall, i.e., $\widehat{y}(t_n)$ as in equation 18:

$$\widehat{y}(t_n) = \widehat{A_J^y}(t_n) + \sum_{j=1}^{J}\widehat{D_j^y}(t_n) = c_0 + \sum_{j=1}^{J}a_{J,i}A_J^{x_i}\left(t_{n-\varsigma_{J,i}}\right) + \sum_{j=1}^{J}\sum_{i=1}^{I}d_{j,i}D_J^{x_i}\left(t_{n-\tau_{j,i}}\right) \quad (18)$$

Where $c_0 = a_{J,1} + d_{j,1}$. Similar to TMLR, the stepwise regression algorithm is performed to select significant predictors from all candidate component variables for WMLR.

3. Empirical Illustration

3.1. Rainfall data:

Indian annual rainfall ranges from less than 1,000 millimeters (mm) in the west to over 2,500 mm in parts of the northeast. All India long term area weighted monthly, seasonal and annual rainfall data from the year 1901 to 2014 is collected from the website (https://data.gov.in/sites/default/files/datafile/All_India_Area_Weighted_Monthly_Seasonal_And_Annual_Rainfall.xls).

3.2. Climate indices:

Selected large-scale climate signals which are related to Indian rainfall for this study are: Indian Ocean Dipole (IOD), and Pacific Decadal Oscillation (PDO). The possible relation between the Indian summer monsoon and the PDO observed in the Sea Surface Temperature (SST) of the North Pacific Ocean. Using long records of observations and coupled model simulation, it has been found that the warm (cold) phase of the PDO is associated with deficit (excess) rainfall over India. The PDO extends its influence to the tropical Pacific and modifies the relation between the monsoon rainfall and El Niño-Southern Oscillation (ENSO). During the warm PDO period, the impact of El Niño (cold period- La Niña) on the monsoon rainfall is enhanced (reduced). Hadley circulation in the monsoon region determines the impact of PDO on the monsoon rainfall. Knowing the phase of PDO may lead to better long-term prediction of the seasonal monsoon rainfall and also the impact of ENSO on monsoon can be known. PDO which is used as a common index for El Ni˜no Southern Oscillation (ENSO), was chosen as a potential predictor of the presence of Indian rainfall. PDO index data is collected from the website- (http://jisao.washington.edu/pdo/PDO.latest).

Variability in the Indian Ocean is associated with variability of rainfall in India, This Variability can be described by Indian Ocean Dipole (IOD) index which is represented by anomalous SST gradient between the western equatorial Indian Ocean (50◦E–70◦E and 10◦S–10◦N) and the south-eastern equatorial Indian Ocean (90◦E–110◦E and 10◦S–0◦N), outgoing longwave radiation, and sea surface height anomalies. This gradient is named as Dipole Mode Index (DMI). When the DMI is positive then, the phenomenon is refereed as the positive IOD and when it is negative, it is refereed as negative IOD. In this study, the DMI index derived from HadISST dataset is also selected as a predictor of the Indian rainfall because it is frequently updated and has a relatively long period of record. The data is obtained from (https://www.esrl.noaa.gov/psd/gcos_wgsp/Timeseries/DMI).

3.3. Implementation and evaluation of the WMLR and TMLR

SAS codes are written for finding the correlation coefficient matrix of Indian annual rainfall and monthly PDO and DMI indices. The procedure begins with the finding of maximum significant correlation (at 5% level of significance) between annual rainfall and monthly indices. Max significant correlated months for each of the indices are selected as potential predictor for fitting the model to predict the annual rainfall. MODWT is carried out on the basis of ‘Haar’ wavelet filter at level 6 to annual rainfall series and the predictor series using R environment. After that each decomposed subseries of rainfall and corresponding different

predictors are fitted into linear regression model. Prediction for those fitted models are obtained and combined for getting the final prediction for rainfall. This whole process involves the WMLR model.

In traditional regression model the monthly indices which are having high and significant correlation (at 5% level of significance) with annual rainfall are selected as predictor variables. Then linear regression model is fitted using R codes. 'Stepwise' algorithm is used for inclusion of those predictors which are significant predictors from all the candidate variables. Prediction on the basis of this model is done and result is obtained.

The Relative Absolute Error (RAE) and correlation coefficient (CC) statistics are used to assess performance of WMLR, in comparison to that of TMLR. The CC shows the degree to which two variables are linearly related. The information about the predictive capability of the models is measured through RAE. The RAE is defined as in equation 19:

$$RAE = \sum_{i=1}^{M} \frac{|Y_{for,i} - Y_{obs,i}|}{Y_{obs,i}} \tag{19}$$

and the correlation coefficient as in equation 20-

$$CC = \frac{\sum_{i=1}^{M} (Y_{obs,i} - \overline{Y}_{obs})(Y_{for,i} - \overline{Y}_{for})}{\sqrt{\sum_{i=1}^{M} (Y_{obs,i} - \overline{Y}_{obs})^2 \sum_{i=1}^{M} (Y_{for,i} - \overline{Y}_{for})^2}} \tag{20}$$

Where $Y_{obs,i}$ and $Y_{for,i}$ stand for observed and forecasted annual rainfall respectively for the i^{th} time step; M is the number of time steps in the test period. $\overline{Y}_{obs}$ and $\overline{Y}_{for}$ stand for mean of observed and forecasted rainfall values, respectively. Both WMLR and TMLR models were trained with the data of 94 -year period (1901-1994). The trained models were used to forecast annual rainfall in test period from 1995 to 2014. Last 20 years data was taken for testing and validation of the newly developed models.

3.4. Results and Discussion

The descriptive statistics of annual rainfall and monthly PDO indices are presented in the Table 1. Same kind of information is obtained for annual rainfall and monthly DMI, which is provided in Table 2. Number of observations is 114 for each of the cases.

Table 1: Descriptive Statistics of all India annual rainfall and monthly PDO indices

Variable	Mean	Std Dev	Minimum	Maximum
ANN	1176	106.65	947.1	1464
JAN	-0.04	1.05	-2.48	2.14
FEB	-0.005	1.06	-3.6	2.07
MAR	0.06	0.97	-2.56	2.41
APR	0.19	0.98	-2.17	2.37
MAY	0.23	0.97	-2.23	2.32
JUN	0.15	1.07	-2.44	3.01
JUL	0.07	1.09	-2.93	3.51
AUG	-0.09	1.05	-2.25	3.31
SEP	-0.17	0.95	-2.28	2.44
OCT	-0.14	0.99	-2.8	2.1
NOV	-0.13	1.05	-3.08	2.65
DEC	0.0007	1.06	-2.75	2.51

Table 2: Descriptive Statistics of Indian annual rainfall and monthly DMI

Variable	Mean	Std Dev	Minimum	Maximum
ANN	1176	106.65	947.1	1464
JAN	0.04	0.25	-0.53	0.69
FEB	0.03	0.26	-0.67	0.72
MAR	0.03	0.25	-0.58	0.62
APR	0.01	0.25	-0.58	0.67
MAY	0.006	0.26	-0.57	0.74
JUN	0.009	0.3	-0.72	0.93
JUL	0.017	0.37	-0.76	1.01
AUG	0.006	0.4	-0.95	1.09
SEP	0.02	0.44	-1.23	1.14
OCT	0.02	0.4	-0.72	1.24
NOV	0.03	0.32	-0.61	1.52
DEC	0.04	0.25	-0.57	1.08

3.5. Significant predictor variables in the WMLR and TMLR models

Correlation coefficient analysis was carried out to obtain indices which were significantly related to annual rainfall. predictors Correlation coefficient of annual rainfall and monthly PDO index is given Table 3.

Table 3: Pearson Correlation Coefficients of ANN and monthly PDO indices

	JAN	FEB	MAR	APR	MAY	JUN	JUL	AUG	SEP	OCT	NEV	DEC

ANN	0.17	0.11	0.11	0.07	0.15	0.07	-0.07	-0.11	-0.23	-0.23	-0.19	-0.24
p-value	0.06	0.23	0.22	0.46	0.10	0.42	0.44	0.22	0.01	0.01	0.03	0.008

From Table 3 it can be found that correlation coefficient of PDO index for September, October and November December months with annual rainfall is significant. So, we can choose indices of any or all of these months as significant predictor variable for forecasting annual rainfall for both the WMLR and TMLR models.

Table 4: Pearson Correlation Coefficients of ANN and monthly DMI, N = 114

	JAN	FEB	MAR	APR	MAY	JUN	JUL	AUG	SEP	OCT	NEV	DEC
ANN	0.04	-0.01	-0.08	-0.05	-0.007	-0.13	0.06	-0.10	-0.27	-0.28	-0.19	-0.11
p-value	0.61	0.90	0.36	0.99	0.53	0.10	0.51	0.26	0.001	0.002	0.04	0.24

From Table 4 it is clear that September, October, November months' IOD index i.e. DMI are significantly correlated with annual rainfall. All the 3 months can be selected as explanatory variable. Important thing is that if you include every month's data for the two predictors discussed above in the model, through stepwise algorithm only significant months for the prediction purpose will be kept.

3.6. Multi Resolution decomposition of rainfall and predictor series

MODWT is carried out on the basis of 'Haar' wavelet filter at level 6. Figure 2(a) represents the 6 wavelet coefficients of annual rainfall in India over 114 years. The most significant PDO index, i.e., the month of December is decomposed through MRA process and presented in Figure 2(b). Similarly, the high correlation of DMI index with the Indian annual rainfall was found for the month of September. September month's DMI index time series data has been decomposed and coefficients are presented in Figure 2(c). The coefficients, i.e., W_1, W_2, W_3, W_4, W_5, W_6 and V_6 are obtained using 'Haar' filter. The graph of W_2 is much smoother than the W_1. Similarly, smoothness increases as we are going to top of the graphs with upper coefficient. In the graph V_6 scaling coefficient shows the smooth lot. This smooth coefficient (V_6) is actual the trend component of signal, hidden in the noisy time series data.

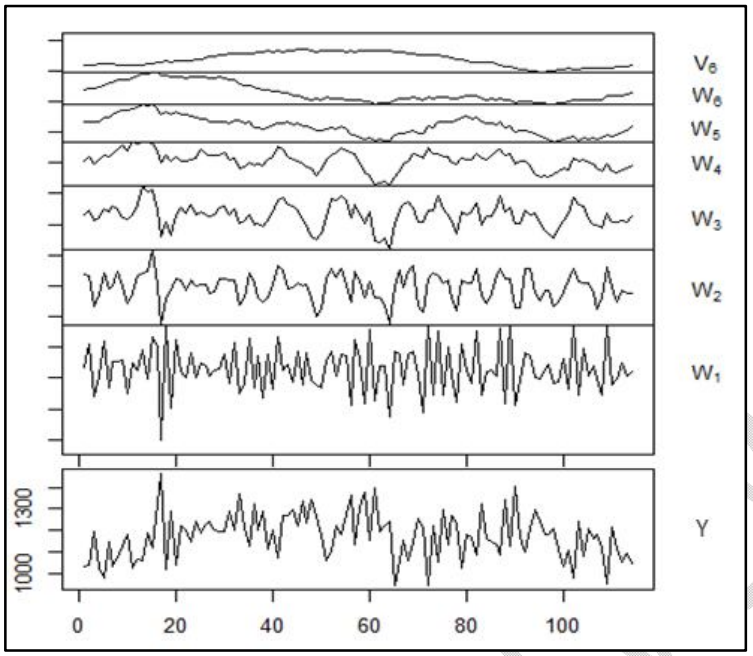

(a)

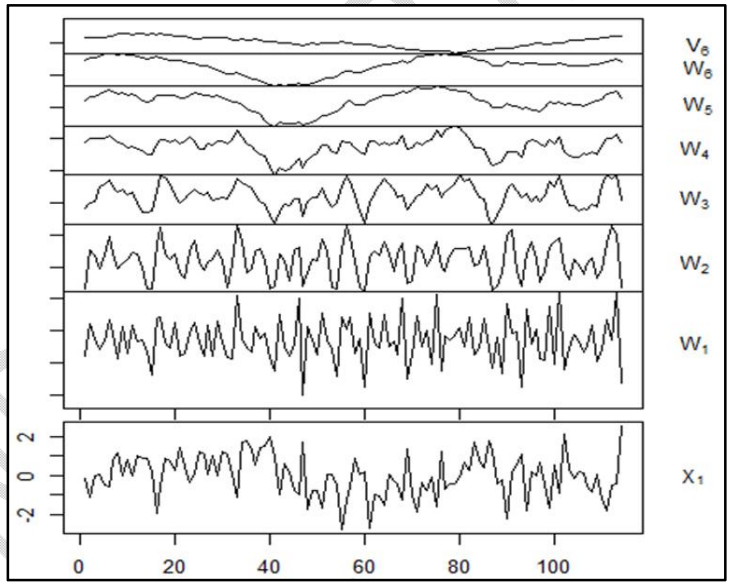

(b)

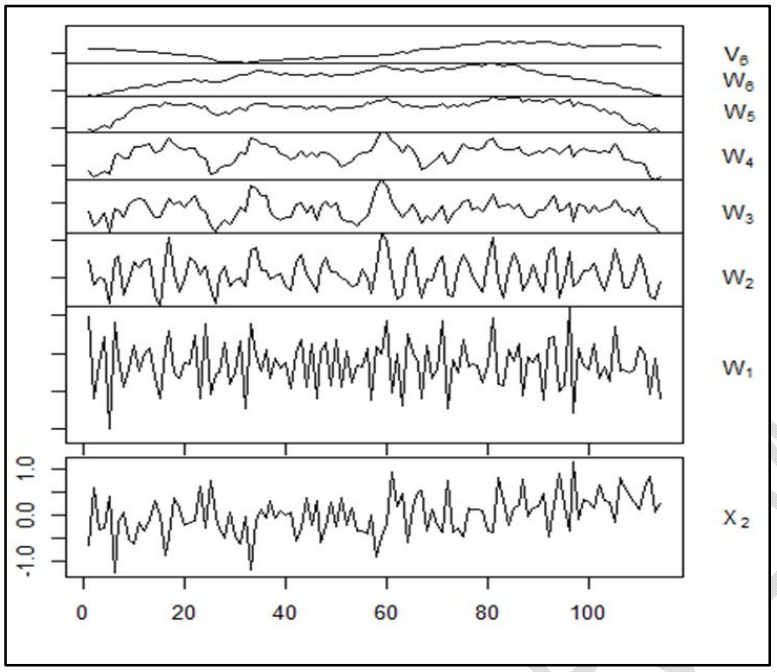

(c)

Figure 2: MODWT plot for (a) annual rainfall, (b) Dec month PDO indices, and (c) Sep month DMI

3.7. Model fitting for WMLR and TMLR model

After decomposing the time series into detail (W) and smooth or approximation(V) component, Maximum LCC (MLCC) are found between predictand and predictor subseries using equation 14. This reveals how strong one predictor subseries is related to the corresponding rainfall subseries. It appears that MRA decomposed series are able to capture more details of rainfall correlations than the original time series. The question is whether they are also useful to improve the rainfall forecasts relative to the original series. This is discussed in subsequent topics. Correlation coefficients between response and predictor variables are given in below tables.

Table 5: Pearson Correlation Coefficients

	PV	DV			DEC (PDO)	SEP (DMI)			PD	DD
RV	-0.21	-0.71		ANN	-0.25	-0.28		RD	-0.36	-0.33
p-Value	0.03	<0.0001		p-Value	0.008	0.003		p-Value	<0.0001	0.0003

(N.B.: RV, PV, DV are indicating smooth component for rainfall, PDO index and DMI; RD, PD, DD are indicating D_1 component for rainfall, PDO index and DMI respectively)

In this study, current year predictor data for the prediction of annual rainfall have been used. Two indices have been used for the prediction purpose. By observing the correlation measures from Table 5, it is clear that decomposition of data increases the correlation between predictor and predictand variables. In WMLR model, after the multi resolution decomposition of rainfall and predictor series predicted value $\widehat{A_J^y}(t_n)$ of the approximation component of rainfall in the highest decomposition level J=6 is obtained through using equation 16. Likewise, predicted value $\widehat{D_j^y}(t_n)$ (j=1,2…6) of the detail components of the rainfall series at each decomposition level j is obtained using equation 17. And finally, combining these forecasted values as in equation 18, we get the forecasted value $\hat{y}(t_n)$ of the rainfall. Similarly, in case of TMLR, original predictor series are used to predict the rainfall. Firstly, predictor variables may be forecasted and those values can be used in the models to get the forecasted rainfall. Forecasted rainfall values from TMLR and WMLR models for the test periods are obtained from equation 15 and equation 18 respectively. Forecasted values by these models have been presented in Figure 3 for visual comparison with the observed rainfall data.

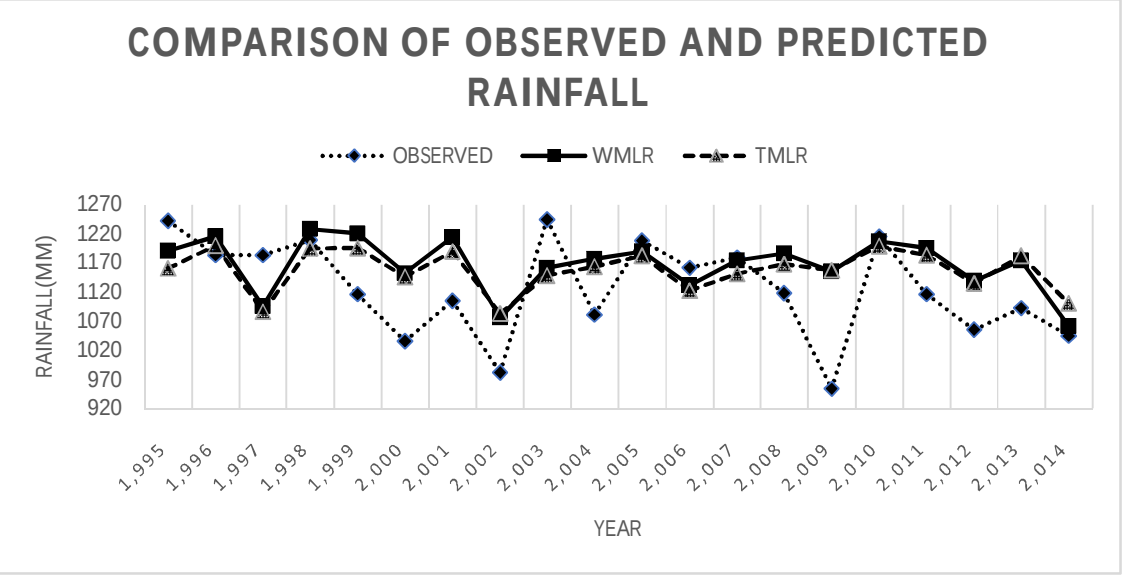

Figure 3: Line chart Comparison between observed and forecasted annual rainfall through WMLR and TMLR models

3.8. Evaluation of the WMLR and TMLR performance

The performance statistics of WMLR and TMLR models are calculated for the test data (1995-2014). RAE values for WMLR and TMLR models are 1.08 and 1.30 respectively. Similarly, CC for these two models are 0.46 and 0.34 respectively. WMLR provides significantly improved accuracy relative to TMLR for annual rainfall forecasts in India. CC from the WMLR is 0.112 points greater than that obtained from TMLR. It can also be found that WMLR model reduces forecast RAE by 1% from the traditional model. So, from RAE and CC viewpoints, the proposed WMLR model performs better than traditional model for forecasting Indian annual rainfall. This may be because the WMLR model has capability to capture the impacts of the predictor variables on the rainfall at different time scales, while the traditional model cannot capture this multiscale information. Although the number of significant predictor variables in the regression based on the decomposition subseries is more than that based on original time series, the original input data for two models are exactly the same. As in the new model the original predictor series are decomposed using MRA, the information contained in the original input data is utilized optimally, leading to an improved forecasting skill. In this study, sixth level of decomposition is used for MRA, with an assumption that most useful information between annual rainfall and potential predictor variables are included within these time scales.

4. Conclusions:

An MRA based MLR model has been presented, tested and discussed for forecasting annual rainfall in Indian scenario. The proposed WMLR combines the MRA for both predictand and candidate predictor variables. The proposed model was trained with the 94-year data, and tested with the remaining 20-year data, and compared to the traditional MLR model based on original time series. The WMLR forecast skill appears to be significantly better than the TMLR model. As DWT is an orthogonal transformation the problem of multicollinearity in the regression problem disappears while using WMLR model. The WMLR model reduced the relative absolute errors by 1% and increased the correlation coefficient by 0.112, in comparison to the TMLR model. Only two indices variables have been used in this study. But there may be many such kind of local or large-scale climate indices which can directly or indirectly explain Indian monsoon rainfall. Therefore, it is open for future research to incorporate many more variables like atmospheric temperature, water vapour, number of sunny days, relative humidity etc. Several other wavelet filters eg., Mexican hat, other Daubechies family of filters (D4, D6, etc.), Symlet, Morlet, B-

Splines, Meyer etc. need to be explored in forecasting rainfall time series data. Notwithstanding, here only one level of decomposition has been used. Therefore, it will be quite interesting to check the effect of multiple levels of decompositions in forecasting performance.

Highlights:

- Large-scale climate indices have been included to improve the rainfall forecasting performance.
- Suitable indices have been chosen using MLCC.
- A new forecasting model based on wavelet decomposition and MLR algorithm (WMLR) has been proposed.
- Empirical study of the newly proposed method has been carried out on Indian annual rainfall.

Software availability

The open-source R-package 'wavelets' developed by Eric Aldrich has been used for present analysis and the package is available for download from the following website https://CRAN.R-project.org/package=wavelets.

COMPETING INTERESTS DISCLAIMER:

Authors have declared that they have no known competing financial interests OR non-financial interests OR personal relationships that could have appeared to influence the work reported in this paper.

Consent for publication: yes

Availability of data and materials: available on request

Compliance with ethical standards

References

Agilan V, Umamahesh N (2018) Covariate and parameter uncertainty in non□stationary rainfall IDF curve. Int J Climatol 38(1):365-383

Archer DR, Fowler HJ (2008) Using meteorological data to forecast seasonal runoff on the River Jhelum Pakistan. J Hydrol 361(1):10–23

Bajirao TS, Kumar P, Kumar M et al (2021) Potential of hybrid wavelet-coupled data-driven-based algorithms for daily runoff prediction in complex river basins. Theor Appl Climatol 145:1207–1231

Beriro DJ, Abrahart RJ, Mount NJ, Nathanail CP (2012) Letter to the Editor on "Precipitation Forecasting Using Wavelet-Genetic Programming and Wavelet-Neuro-Fuzzy Conjunction Models" by Ozgur Kisi & Jalal Shiri. Water Resour Manag 26(12)3653–3662

Burrus CS, Gopinath RA, Guo H (1998) Introduction to wavelets and wavelet transforms: a primer Prentice-Hall

Burt P, Adelson E (1983a) The Laplacian pyramid as a compact image code. IEEE Trans Commun 31:482-540

Burt P, Adelson E (1983b) A multiresolution spline with application to image mosaics. ACM Trans Graph 2:217-236

Buttinger-Kreuzhuber A, Konev A, Horváth Z, Cornel D, Schwerdorf I, Blöschl G, Waser J (2022) An integrated GPU-accelerated modeling framework for high-resolution simulations of rural and urban flash floods. Environ Model Softw 156:105480

Coon ET, Shuai P (2022) Watershed Workflow: A toolset for parameterizing data-intensive integrated hydrologic models. Environ Model Softw 105502

Daubechies I (1992) Ten Lectures on Wavelets SIAM Philadelphia

Draper NR, Smith H (1998) Applied Regression Analysis Wiley- Inter-science: Hoboken

de Andrade Lima Neto E, Pinheiro A, Gomes de Oliveira Ferreira A (2021) On wavelet to select the parametric form of a regression model. Comm Statist Simulation Comput 50(9):2619-2642

Delsole T, Shukla J (2012) Climate models produce skilful predictions of Indian summer monsoon rainfall. Geophys Res Lett 39:L09703

Demir V (2022) Enhancing monthly lake levels forecasting using heuristic regression techniques with periodicity data component: application of Lake Michigan. Theor Appl Climatol 148:915–929

Fahimi F, Yaseen ZM, El-shafie A (2017) Application of soft computing-based hybrid models in hydrological variables modeling: a comprehensive review. Theor Appl Climatol 128:875–903

Ghosh H, Paul RK, Prajneshu (2010) Wavelet Frequency Domain Approach for Statistical Modeling of Rainfall Time-Series Data. J Stat Theory Pract 4(4):813-825

Jeong C, Shin JY, Kim T, Heo JH (2012) Monthly precipitation forecasting with a neuro-Fuzzy model Water Resour Manag 26(15):4467–4483

Jeong J, Park E, Chen H, Kim KY, Han WS, Suk H (2020) Estimation of groundwater level based on the robust training of recurrent neural networks using corrupted data. J Hydrol 582:124512

Jia X, Shao M, Zhu Y, Luo Yi (2017) Soil moisture decline due to afforestation across the Loess Plateau China. J Hydrol 546:113–122

Jiang Z, Sharma A, Johnson F (2020) Refining predictor spectral representation using wavelet theory for improved natural system modeling. Water Resour Res 56(3):e2019WR026962

Jiang Z, Rashid MM, Johnson F, Sharma A (2021) A wavelet-based tool to modulate variance in predictors: An application to predicting drought anomalies. Environ Model Softw 135:104907

Gao S, Huang Y, Zhang S, Han J, Wang G, Zhang M, Lin Q (2020) Short-term runoff prediction with GRU and LSTM networks without requiring time step optimization during sample generation. J Hydrol 589:125188

Goupillaud P, Grossmann A, Morlet J (1984) Cycle-octave and related transforms in seismic signal analysis. Geoexploration 23(1):85–102

Karbasi M, Karbasi M, Jamei M et al (2022) Development of a new wavelet-based hybrid model to forecast multi-scalar SPEI drought index (case study: Zanjan city Iran). Theor Appl Climatol 147:499–522

Karumuri A, Hameed S (2007) On impacts of ENSO and Indian Ocean Dipole events on the sub-regional Indian summer monsoon rainfall. Nat Hazards 42:273-285

Kim Y, Shin HS, Plummer JD (2014) A wavelet-based autoregressive fuzzy model for forecasting algal blooms. Environ Model Softw 62:1-10

Krishnamurthy L, Krishnamurthy V (2012) Influence of PDO on South Asian summer monsoon and monsoon–ENSO relation. Clim Dyn 42:9-10

Kusiak A, Verma AP, Roz E (2013) Modeling and prediction of rainfall using radar refectivity data: a data-mining approach. IEEE Trans Geosci Remote Sens 51:2337–2342

Lim E, Hendon H, Hudson D, Wang G, Alves O (2009) Dynamical forecast of inter-El Ni˜no variations of tropical SST and Australian spring rainfall. Mon Weather Rev 137(11):3796–3810

Lindsay RW, Percival DB, Rothrock DA (1996) The discrete wavelet transforms and the scale analysis of the surface properties of sea ice. IEEE Trans Geosci Remote Sens 34:771–787

Liyew CM, Melese HA (2021) Machine learning techniques to predict daily rainfall amount. J Big Data 8153

Mallat S (1989) A theory for multiresolution signal decomposition: the wavelet representation IEEE Trans Pattern Anal Mach Intell 11:674–693

Makridakis S, Anderson A, Carbone R, Fildes R, Hibdon M, Lewandowski NJ, Parzen E, Winkler R (1982) The accuracy of extrapolation (time series) methods: results of a forecasting competition. J Forecast 1:111-153

Mart´ınez B, Gilabert M (2009) Vegetation dynamics from NDVI time series analysis using the wavelet transform. Remote Sens Environ 113:1823–1842

Meinke H, Stone R (2005) Seasonal and interannual climate forecasting: the new tool for increasing preparedness to climate variability and change in agricultural planning and operations. Clim Change 70:221–253

Mutai C, Ward M, Colman A (1998) Towards the prediction to the East Africa short rains based on the Sea Surface Temperature – Atmospheric Coupling. Int J Climatol 18:975–997

Paul RK, Birthal PS (2016) Investigating rainfall trend over India using the wavelet technique J Water Clim Chang 7(2):353-364

Paul RK, Paul AK, Bhar LM (2019) Wavelet-based combination approach for modeling sub-divisional rainfall in India. Theor Appl Climatol 139(3):949-963

Paul RK, Garai S (2021) Performance comparison of wavelet-based machine learning technique for forecasting agricultural commodity prices. Soft Comput 25:12857–12873

Paul RK, Garai S (2022) Wavelets Based Artificial Neural Network Technique for Forecasting Agricultural Prices. J Ind S Prob Stat 23:47-61

Percival DB, Walden AT (2000) Wavelet methods for time series analysis Cambridge University Press. Cambridge, UK

Prasad K, Dash SK, Mohanty UC (2010) A logistic regression approach for monthly rainfall forecasts in meteorological subdivisions of India based on DEMETER retrospective forecasts. Int J Climatol 30(10):1577–1588

Quilty J, Adamowski J (2021) A maximal overlap discrete wavelet packet transform integrated approach for rainfall forecasting–A case study in the Awash River Basin (Ethiopia). Environ Model Softw 144:105119

Rashid A, Alamgir M, Ahmed MT et al (2022) Assessing and forecasting of groundwater level fluctuation in Joypurhat district northwest Bangladesh using wavelet analysis and ARIMA modeling. Theor Appl Climatol 150:327–345

Ray M, Singh KN, Ramasubramanian V, Paul RK, Mukherjee A, Rathod S (2020) Integration of wavelet transform with ANN and WNN for time series forecasting: an application to Indian monsoon rainfall. Natl Acad Sci Lett 43(6):509-513

Sahai AK, Soman MK, Satyan V (2000) All India summer monsoon rainfall prediction using an artificial neural network. Clim Dyn 16:291–302

Schepen A, Wang Q, Robertson D (2012) Combining the strengths of statistical and dynamical modeling approaches for forecasting Australian seasonal rainfall. J Geophys Res 117:D20107

Schneider JM, Garbrecht JD (2003) A measure of the usefulness of seasonal precipitation forecasts for agricultural applications. Trans ASAE 46(2):257–267

Sharma A (2000) Seasonal to interannual rainfall probabilistic forecasts for improved water supply management: part 3—a nonparametric probabilistic forecast model. J Hydrol 239(1):249–258

Singh SK, Griffiths GA, Pham HX (2021) Meteorological drought in Northland New Zealand: a regional and local analysis using copulas. J Hydrol 60:1-16

Tezel G, Buyukyildiz M (2016) Monthly evaporation forecasting using artificial neural networks and support vector machines. Theor Appl Climatol 124:69–80

Tessier Y, Lovejoy S, Hubert P, Schertzer D, Pecknold S (1996) Multifractal analysis and modelling of rainfall and river flows and scaling causal transfer functions. J Geophys Res 101(D21):26427–26440

Thirumalai C, Harsha KS, Deepak ML, Krishna KC (2017) Heuristic prediction of rainfall using machine learning techniques. International Conference on Trends in Electronics and Informatics (ICEI) IEEE: New York 1114–1117

Ummenhofer C, England M, McIntosh P, Meyers G, Pook M, Risbey J, Gupta A, Taschetto A (2009) What causes southeast Australia's worst droughts? Geophys Res Lett 36:L0

Vijayan R, Mareeswari V, Mohankumar P, Gunasekaran G, Srikar K (2020) Estimating rainfall prediction using machine learning techniques on a dataset. Int J Sci Technol Res 9(06):440–5

Yucel I, Onen A, Yilmaz K, Gochis D (2015) Calibration and evaluation of a flood forecasting system: Utility of numerical weather prediction model data assimilation and satellite-based rainfall. J Hydrol 523:49–66

Zhang J, Zhu Y, Zhang X, Ye M, Yang J (2018) Developing a long short-term memory (LSTM) based model for predicting water table depth in agricultural areas. J Hydrol 561:918–929

Zeelan BCMAK, Bhavana N, Bhavya P, Sowmya V (2020) Rainfall prediction using machine learning & deep learning techniques Proceedings of the International Conference on Electronics and Sustainable Communication Systems (ICESC 2020) Middlesex University: IEEE Xplore 92–97